FINAL TECHNICAL REPORT
Title Page

Project Title: The Incubation of Next-Generation Radar Technologies to Lower the Cost of Wind Energy

Recipient: Texas Tech University, DUNS#: 041367053
Award Number: DE-EE0006804
Project Period: 12/15/2014-03/15/2017

Principle Investigator: John Schroeder, Professor of Atmospheric Science, john.schroeder@ttu.edu, 806-834-5678

Federal Agency to which Report is submitted: DOE EERE – Wind & Water Power Program
Date of Report: March 15, 2017

Working Partners: NA
Cost-Sharing Partners: NA

ACKNOWLEDGMENT AND DISCLAIMER

Acknowledgment: This report is based upon work supported by the U. S. Department of Energy under Award No. DE-EE0006804.

Disclaimer: Any findings, opinions, and conclusions or recommendations expressed in this report are those of the author(s) and do not necessarily reflect the views of the Department of Energy.

CONTENTS

LIST OF ACRONYMS

AWEA – American Wind Energy Association
DOE – U. S. Department of Energy
DOE-X – U. S. Department of Energy X-Band Radar Prototype
HVAC – Heating, Ventilation, and Air Conditioning
IF – Intermediate Frequency
IP – Intellectual Property
LIDAR – LIght Detection And Ranging
LNA – Low Noise Amplifier
NEPA – National Environmental Policy Act
NetCDF – Network Common Form Data
NEXRAD – Next-Generation Weather Radar used by the National Weather Service
NWI – National Wind Institute
PPI – Plan Position Indicator
PRF – Pulse Repetition Frequency
QA/QC – Quality Assurance/Quality Control
RADAR – RAdio Detection And Ranging
RHI – Range Height Indicator
RF – Radio Frequency
SCADA – Supervisory Control and Data Acquisition
SQI – Signal Quality Index
SWiFT – Scaled Wind Farm Testing Facility/DOE
TRL – Technology Readiness Level
TTU – Texas Tech University
TTUKa – Texas Tech University Ka-Band Radar
TWT – Traveling Wave Tube
UPS – Uninterruptible Power Supply
UTC – Coordinated Universal Time

LIST OF FIGURES

LIST OF TABLES

EXECUTIVE SUMMARY

The National Wind Institute (NWI) at Texas Tech University (TTU) has had an impressive and well documented 46-year history of wind related research activities (http://www.depts.ttu.edu/nwi/). In 2011 with funding from the United States Department of Energy (DOE), an NWI team applied radar technologies and techniques to document the complex flows occurring across a wind plant. The resulting efforts yielded measurements that exceeded the capabilities of commercial lidar technologies with respect to maximum range, range resolution and scan speed. The NWI team was also the first to apply dual-Doppler synthesis and objective analysis techniques to resolve the full horizontal wind field (i.e. not just the line-of-sight wind speeds) to successfully define turbine inflow and wake flows across large segments of wind plants. While these successes advanced wind energy interests, the existing research radar platforms were designed to serve a diversity of meteorological applications, not specifically wind energy. Because of this broader focus and the design choices made during their development, the existing radars experienced technical limitations that inhibited their commercial viability and wide spread adoption.

This DOE project enabled the development of a new radar prototype specifically designed for the purpose of documenting wind farm complex flows. Relative to other "off the shelf" radar technologies, the specialized transmitter and receiver chains were specifically designed to enhance data availability in non-precipitating atmospheres. The new radar prototype was integrated at TTU using components from various suppliers across the world, and installed at the Reese Technology Center in May 2016. Following installation, functionality and performance testing were completed, and subsequent comparative analysis indicated that the new prototype greatly enhances data availability by a factor of 3.5-50 in almost all atmospheric conditions. The new prototype also provided enhanced signal quality in clear air (i.e. non-precipitating) environments, mitigated atmospheric attenuation, and extended the useful range of data collection to beyond 30km in cooperative atmospheric conditions. Additionally, the new DOE-X prototype was shown to benefit from Bragg scattering when the thermal stratification of the atmosphere is strong (i.e. nocturnal hours). This result was not possible in any capacity with the previous technology. Combined, these developments represent the achievement of all project objectives, advance the Technical Readiness Level (TRL) to a level of 7, and open the door for more widespread adoption and usage in the wind energy sector. At the same time, radar induced artifacts from multi-trip echoes and ground targets increased with the new technology, and these required additional attention for some applications.

Commercialization activity accelerated in parallel with the DOE funded project, as SmartWind Technologies, L.L.C., was contracted to provide two new radar systems to DONG Energy to monitor the Westermost Rough wind plant off the east coast of the United Kingdom. These new early stage commercial radars systems were closely related to the DOE prototype, but maintain more robust ancillary support systems. The radars were installed during the summer of 2016, and have been operational since that time. Additionally, commercially funded advancements have since been made in processing sophistication to mitigate the previously identified radar artifacts. TTU and SmartWind Technologies stand ready to provide public and private partners focused on wind plant optimization with this new capability. Ancillary interests have also been identified as the initial deployments of the technology have shown the ability to identify and track avian and drone activity, opening up multi-purpose operational opportunities.

INTRODUCTION

The goal of this project is to revolutionize wind farm complex flow measurements. The newly developed prototype (i.e. the DOE-X radar) will assist the United States Department of Energy (DOE) and industry partners to develop smart wind farms, where energy extraction and the mitigation of turbine loads at a wind plant scale are targeted. By providing reliable complex flow information at sufficient resolution from across an entire wind plant, the new radar technology opens the door for the rapid advancement of wind plant scale control concepts. Given that there is up to a 30% reduction [1] in plant performance due to turbine-to-turbine interaction alone (Figure 1), new optimization concepts at the plant level offer a tremendous opportunity to enhance the output from new and existing wind plants and significantly lower the cost of energy. The developed radar prototype provides a cornerstone instrument to help design and validate these optimization concepts.

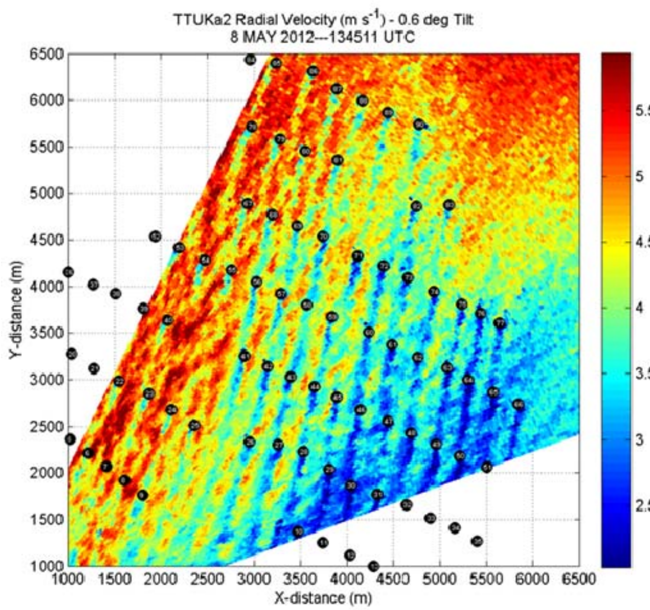

Figure 1. Image of radial velocities measured across the broad region of an operational wind plant using the TTUKa research radars.

The vast majority of operational wind turbines operate in a completely reactive state without any knowledge of the pending inflow or the generated wake flow. If remote sensing is employed (typically via look ahead lidar), it is almost exclusively focused on enhancing "limited" inflow knowledge to an *individual turbine*. In contrast, the new DOE-X prototype will provide access to foundational *wind plant* complex flow information that enables a system level focus on turbine-to-turbine interaction and wind plant optimization. Currently, no other remote sensing technology has the potential to contribute as broadly at this scale.

The feasibility of employing radar technology to measure wind plant relevant complex flows (e.g. turbine-to-turbine interaction, turbine wakes, and wind plant edge effects) was historically proven by the NWI team using the TTUKa radars. However, the pre-existing radar technology could only provide limited data availability in many non-precipitating environments (i.e. clear air), did not operate in an autonomous manner, was susceptible to attenuation in moderate/heavy precipitation, and exhibited water vapor and sea salt absorption issues that minimized performance offshore. While maintaining adequate spatial and temporal resolution, the new DOE-X prototype operates at a different wavelength, with higher peak output power, and a highly customized receiver chain to afford a substantial improvement in clear air data availability. This result includes a significant contribution from Bragg scattering during nocturnal hours when the atmosphere harbors strong temperature gradients in the lower levels. Given their millimeter wavelength, Bragg scattering did not contribute to the TTUKa radars in any meaningful way. The ability to operate using a lower pulse repetition frequency and achieve equivalent or better data availability also provides an extended range capability useful for monitoring wind plant adjacent flows and even plant-to-plant interaction. Finally, the automation of basic quality assurance/quality control (QA/QC) functionality and production of user-friendly Network Common Data Format (NetCDF) file structures provide for quicker downstream integration by users.

Prior to the start of this project, TTU had signed an exclusive license agreement with SmartWind Technologies, LLC for use of the previously developed foundational intellectual property (IP). This IP (i.e. using radar technologies and dual-Doppler synthesis techniques for wind plant complex flow measurement) was generated from a previous DOE award (FG36-06GO86092), and resulted in two US patents (9,519,056 and 9,575,177). During this project, the commercialization process advanced as SmartWind Technologies was contracted by DONG Energy to develop and install a set of two radar systems for monitoring of the Westermost Rough offshore wind plant located adjacent to the east coast of the United Kingdom. These early stage commercial systems are similar in design to the new DOE-X prototype, but maintain more advanced ancillary support systems (e.g. full battery backup, communications links, processing servers, etc.). The two new radar systems were installed summer 2016, and the measurements were combined to provide dual Doppler synthesis of the wind plant complex flows. To achieve success in the commercial application, more sophisticated signal processing and post processing algorithms have been developed to address radar artifacts emanating from the wind turbines themselves, multi-trip echoes, and sea clutter influences. TTU and SmartWind Technologies have now proven that this next generation radar technology can serve the future marketplace by developing complementary hardware and software solutions focused on resolving wind plant relevant complex flow fields.

BACKGROUND

Previous Wind Plant Complex Flow Measurements

The NWI at TTU has an impressive and well documented 46-year history of wind related research activities (http://www.depts.ttu.edu/nwi/). More recently, an NWI team has applied radar technologies (Figure 2) [2] and techniques [3] to measure complex flows across wind plants [4, 5, 6] (Figure 3), document wind ramp events [7], and examine wake steering concepts [8]. Additional efforts related to developing more detailed approaches to define high-resolution wind turbine inflow and wake flow conditions (i.e. wind speed, wind direction, veer, shear, and turbulence), forecasting inflow conditions up to 60-90 seconds in advance, and detailing the impact of rapidly changing atmospheric stability states on wind turbine/plant operations is currently ongoing with support from the National Science Foundation. Additional efforts funded by the DOE have also focused on verification and validation [9]. The NWI team was the first to apply dual-Doppler synthesis and objective analysis techniques to resolve the full horizontal wind field (i.e. not just the line-of-sight wind speeds) at relevant scales to define turbine inflow and wake flows across wind plants, and now they have been focused on advancing the technology and the method to broaden its application.

Figure 2. Image of a TTUKa radar deployed adjacent to an operational wind plant.

The NWI team's usage of specialized radar technology for documenting wind plant complex flows helps to unlock our understanding of turbine-to-turbine interaction, provide validation for industry and academic-led wind tunnel experimentation and numerical modeling efforts, refine the engineering design of wind turbines and their foundations, and provide fundamental information to assist in the development of proactive wind plant level controls (e.g. wake management). This wealth of wind flow knowledge was not previously available.

While these successes were beneficial, the existing research radar platforms (i.e. the TTUKa radars) were designed to serve a diversity of meteorological applications (e.g. severe storms research). Because of design choices, there were technical limitations in the TTUKa systems that needed to be mitigated to allow broader application in the wind energy industry. NWI has worked closely with several industry partners to deploy the existing TTUKa systems in support of wind plant complex flow measurements. The feedback from these projects has been consistent:

- The collected TTUKa radar measurements are rich with detail and surpass measurements collected using any other available remote sensing technology.
- The dual-Doppler synthesized TTUKa wind speed and direction values compare well with in-situ towers, vertically pointing lidars and other technologies.
- The clear air sensitivity of the TTUKa technology must be improved upon to allow more reliable performance in a wider range of atmospheric conditions.
- Ease of unit operation, deployment and subsequent analyses must be substantially improved for non-expert users.

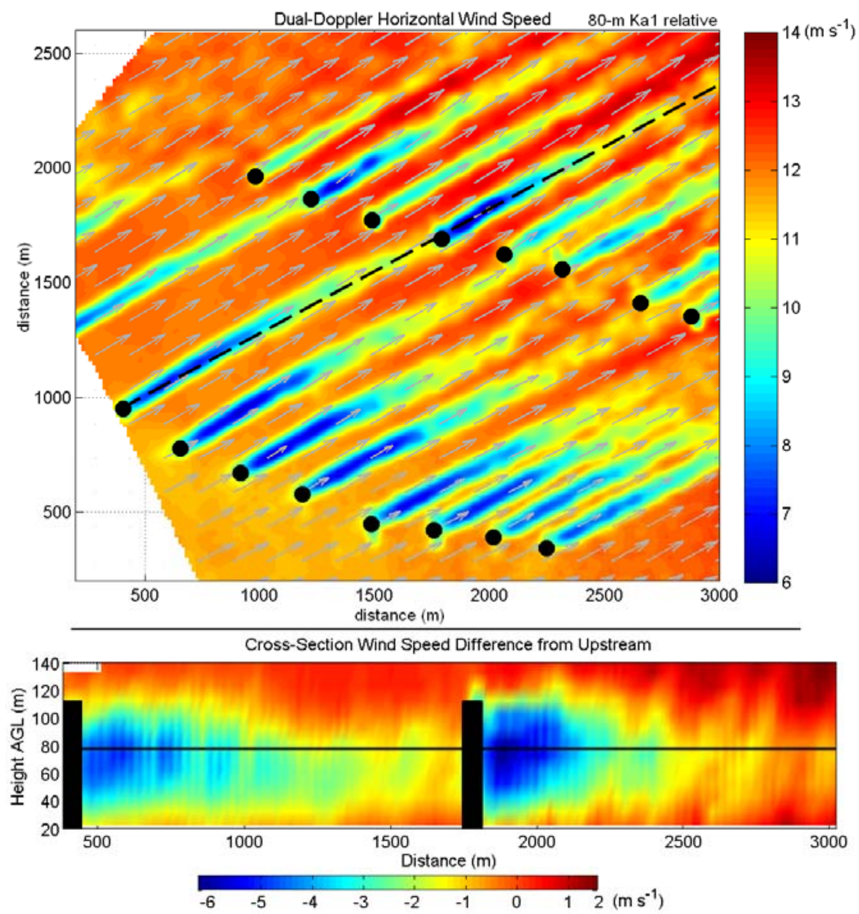

Figure 3. Horizontal cross section at hub height (top) and vertical cross section (bottom) of dual-Doppler synthesized horizontal wind field.

Hence, the primary objective of this project was to develop a commercially viable radar prototype to serve the wind energy industry's need to measure and document wind plant complex flow fields. To effectively complete this objective, the identified weaknesses of the existing TTUKa radars needed to be mitigated, while the appropriate spatial and temporal resolutions were preserved to support the measurement of the relevant scales of motion and the optimal completion of dual-Doppler synthesis.

Comparison to Available Commercial Technologies

A reasonable question to ask is why existing commercial technologies cannot fill the intended role of the new DOE-X radar prototype developed under this project. Fundamentally, the capabilities of any remote sensing technology will vary by design and environmental conditions, which can lead to many technologies being complementary, especially when considering a wide array of measurement objectives. However, for the purposes of the following comparative discussion, the focus is on the measurement of wind plant complex flow fields to assist in the development of enhanced wind plant controls.

Scanning Lidar

Although LIght Detection And Ranging (lidar) and RAdio Detection And Ranging (radar) share some common terminology, there are intrinsic differences in their excitation and detection methods. Commercial lidar has been "matured" for application in the wind energy industry, but the majority of the market sector is focused on limited "look-ahead" techniques for defining individual wind turbine inflow conditions or constructing single vertical wind profiles for resource assessment (e.g. virtual meteorological mast). Scanning lidars offer the closest match to the capabilities of a scanning radar system, but there are distinct differences that impact the ability to synthesize the resultant measurement fields at the required scales of motion to document wind plant complex flows.

Conventional lidar systems typically use a Fabry-Perot etalon interferometer technique in which the excitation source, nominally eye-safe infrared laser light, is emitted to the target in either a pulsed or continuous fashion. The targets, air molecules and aerosol scatterers, then reflect a small portion of this light back to an optical telescope system. In contrast, conventional radar systems utilize a radio frequency (RF) signal that is transmitted to the target, scattered and then received via a highly focused scanning antenna system. The target in this case can be aerosols, water vapor or water droplets. The return signal is demodulated electronically in order to recover the target magnitude, phase and spectral characteristics. For comparison, we consider a state-of-the-art scanning lidar, specifically the Lockheed Martin developed WindTracer. Table 1 provides a comparison between the DOE-X prototype developed using this award and the Wind Tracer based on available documentation acquired in 2013 from the website http://www.lockheedmartin.com/us/products/windtracer.html.

Performance in Varied Atmospheric Environments

For the WindTracer lidar system, which operates at a wavelength of 1.617µm, the optimal operating atmospheric environment is dry clear air with sufficient molecular scattering density. The performance can be reduced in damp to moderate precipitating conditions. In comparison, the new DOE-X prototype operates at a wavelength of ~3.2cm, with optimal operating atmospheric environments of clear air with well mixed particulate scattering density (or Bragg scattering) to heavy precipitation. The performance can be reduced in some clear air environments or attenuated in severe precipitating conditions (e.g. hail). The degree to which the DOE-X prototype operates in non-precipitating environments is addressed later in this report, but based on published reports, the lidar technology will likely produce more data availability in some non-precipitating atmospheres out to ranges of ~10 km, while the radar will provide more information in some non-precipitating environments as well as during precipitation.

Maximum Range

For the WindTracer lidar system, the maximum range is 15 km, and the useable range in many atmospheres will be less. The DOE-X prototype operates using a pulse repetition frequency (PRF) of 4,000 Hz when using a 20 µsec compressed pulse. This PRF allows a maximum range of approximately 35 km, while the usable range of the radar will also vary with atmospheric conditions. The longer maximum range enables several possibilities, including campaigns that couple wind plant complex flow measurements with longer range studies focused on documenting plant-to-plant influences.

Spatial Resolution

When employing pulse compression techniques, the return target signature to the DOE-X prototype is contained within a narrow, frequency domain bandwidth, which yields enhanced range resolutions (typically between 9-15 m) relative to any commercially available lidar system (typically 60 m). While the azimuthal beam spread of the DOE-X prototype (0.49° half power beam width) cannot be avoided, the relative balance between the azimuthal and range resolutions at many ranges (e.g. 3-10 km) provides for more optimal dual-Doppler syntheses. Lidar's pencil beam volume provides excellent azimuthal resolution, but relatively coarse range resolution (especially at greater ranges), providing for a less balanced synthesis when multiple look angles are incorporated. If the measurement objective is focused on extracting average flow conditions over a 10-minute period, this difference will not likely significantly influence the analysis result. On the other hand, if the measurement objective is focused on extraction of boundary layer flow features on the scale of the rotor size or smaller (i.e. temporal scales over the course of seconds), this difference may yield a less suitable analysis.

Table 1. Comparison of the WindTracer[1] Doppler lidar and DOE-X prototype.

Parameter	WindTracer Doppler Lidar	DOE-X Prototype Radar
Transmit Wavelength	Eye safe infrared, 1617ηm	Eye Safe Microwave, 3.2cm
Measurement Range	400m to 15km	Conventional pulse: 0 to 20km; Pulse Compression: 2.5km to 30km
Radial Wind Velocity Range	+/- 38m/s	Nyquist as per PRF, multiple PRF unfolding possible
Velocity Accuracy	Radial velocity; <0.5m/s to 0.1m/s for high SNR	Radial velocity; 0.03m/s
Minimum Range Resolution[2]	60.0m	9.0m
Beam Diameter	9.6cm (e^{-1} intensity width)	0.49° half power beam width
Gridded Data Resolution	100m Cartesian grid output, 5-10m Vertical	10m Cartesian grid output, 2-5m Vertical
Volumetric Update Rate	5 to 10 minutes, site specific dependency	Full Volume PPI: 55-80 seconds Single 360 degree scan: 12 seconds Single RHI: 0.8-1.2 seconds
Azimuth Range	0 to 360°	0 to 360°
Elevation Range	-5 to 185°	-3 to 90°
Pointing Accuracy	+/- 0.1°	+/- 0.05°
Pulse Duration	300ηsec +/- 150ηsec	Variable from 100ηsec conventional pulse to 20μsec pulse compression
Pulse Repetition Frequency	750 Hz	Variable from 300 to 4,000 Hz

[1]WindTracer statistics acquired from online documentation in 2013, except where otherwise noted.
[2]WindTracer minimum range resolution updated based on 2014 AWEA WindPower Presentation by Justin Sharp.

Temporal Resolution

Temporal resolution (i.e. scan speed) is also important for measuring the evolution of wind plant complex flows, and lidar is limited relative to radar technologies in this facet. Radar scan rates are nominally set to approximately 30°/second, while the lidars scans at approximately 1-3°/second. Hence, revisit times (i.e. the time it takes between volume samples) are significantly reduced (i.e. an order of magnitude) for radars for any given domain. For instance, a nominal scanning volume covering a large turbine array through the depth of the rotor sweep might be collected in one minute by a radar rather than 10-minutes by a lidar. Hence, scanning lidars struggle to provide adequate measurements for multi-look volume-based synthesis techniques. Smaller scale boundary layer features translating in the background flow field are of interest to wind turbine and wind plant controls development, but would be difficult to resolve in an equivalent volume across a broader region using a scanning lidar. It should be noted that in challenging atmospheric conditions with minimal scatterer density, a radar's scan rate can also be decreased significantly to operate more like a scanning lidar. This reduction in scan speed greatly enhances sample size for any given bin and effectively increases data availability, but similarly compromises the use of dual-Doppler synthesis and the wind flow scales that can be resolved.

Lidar Summary

Published scanning lidar based studies typically include line-of-site velocities focused on an individual or a small collection of turbine wakes across a limited measurement domain, or measurements from a broader domain where smaller scales of motion are unimportant to document and longer temporal averaging can be employed. Dual-lidar information from a large wind turbine array showing smaller scales of motion is not currently available. Radar on the other hand, has been used to examine flow structures across larger domains, and can offer rapid revisit times and dual-Doppler synthesis supporting documentation of smaller scales of motion and transient, high-impact wind events. Fundamentally, a lidar is better suited for measurement objectives where longer temporal averaging and data availability is stressed (e.g. resource assessment), while radar is better suited for campaigns stressing small scale flow evolution and/or larger experimental domains. In many ways, the two technologies can serve different, but complementary purposes.

Discussion of other Radar Technologies

Other X-band weather radar systems are available "off the shelf." However, these systems are exclusively geared toward weather detection. While one of the most advanced and widely used dual-polarization X-band weather radar systems on the market today is an exceptional unit for weather detection and supports many advanced features for that application, it has several limitations that prohibit its use in wind plant complex flow detection and analysis. Two critical factors for wind plant application are data availability in a clear-air environment and high resolution.

The comparative system uses a magnetron oscillator based transmitter which is limited in duty cycle to 0.5% and cannot be modulated to produce a compressed pulse. The DOE-X band system uses a novel technique to combine two traveling wave tube (TWT) amplifiers, which support complex pulse-compression modulation, and provide an overall 8.0% duty cycle. Leveraging the high duty cycle along with pulse compression techniques affords this system with almost 2 orders of magnitude additional signal-to-noise ratio sensitivity over a conventional magnetron based weather radar system. In addition, custom designed high-order matched analog ceramic filter networks within the DOE-X band receiver system provide precise multi-channel simultaneous up/down conversion of the non-linear FM pulse compression modulation scheme in order to maintain spectral purity/integrity of the complex modulation pulse and corresponding target return.

The comparative system utilizes a 1.0° beam width parabolic reflector, which is adequate for long range weather detection and analysis. However, in order to achieve the high azimuthal resolution required to accurately sample the complex flow environment within a wind plant, the DOE-X band system utilizes a 0.5° beam width parabolic reflector.

RESULTS AND DISCUSSION

Project Objectives

This project was focused on advancing the use of radar technology for measuring wind plant complex flows. In particular, the project objectives were to address the identified weakness of the existing TTUKa radar technology. Since the TTUKa radars represented the existing state-of-the-art technology available in the scientific literature prior to the start of this project, the capabilities of the TTUKa radars are used as a baseline to gauge improvement of the new DOE-X prototype.

Enhancing data availability in a wider range of atmospheric environments was the highest priority objective, as it addressed the most fundamental weakness associated with the TTUKa radars. An increase in data availability would result in an immediate reduction in the time necessary to achieve experimental goals, yielding an immediate benefit and expanded application. To accomplish this objective, system enhancements would be required to increase the system sensitivity in clear-air (i.e. non-precipitating) environments, as well as mitigate the atmospheric attenuation and absorption that are known to be limitations at the Ka-band. This improved data availability would have to be achieved without sacrificing spatial and/or temporal resolution, as they are required for dual-Doppler synthesis to yield analysis of the relevant scales of motion (i.e. rotor scale and smaller).

From past experience and interactions with industry, operating the current TTUKa radar technology and/or working with the raw data produced by the systems is difficult for untrained individuals. Hence, the implementation of real-time file format conversion to a generic NetCDF format and first-order editing procedures was a secondary project objective. Meeting this objective would also minimize the steps required to develop relevant downstream industry products (e.g. generated inflow time histories for a set of turbines, wake deficit cross-sections, etc.).

Finally, the TTUKa research radars require almost constant interaction with an operator, which isn't cost effective or feasible for a long-term deployment at a wind plant. The new DOE-X prototype was to be designed and configured to operate in a far more autonomous manner, thereby enabling long term deployments without constant user interaction.

Targeted Performance Metrics

Against the backdrop of these identified project objectives, the target performance metrics for the DOE-X prototype radar were established. Table 2 provides a comparison of the existing TTUKa and the proposed DOE-X prototype specifications, and the related performance metrics.

Data Availability

Data availability improvements were expected due to a DOE-X system design which yielded an enhanced Rayleigh scattering regime, more power to the target, and a significant reduction in return signal loss within the receiver chain. Many of these improvements were already known in advance and are based on established principles of radar engineering, but the collective improvement in system data availability was assessed through performance testing relative to a TTUKa radar.

Frequency/Wavelength Changes

Given conducive atmospheric conditions for backscattering in the 35 GHz (Ka) band, such as lightly precipitating environments or clear-air/non-precipitating environments with ample particulate scattering density, the TTUKa systems performed exceptionally well and afforded noise-free coherent Doppler velocity measurements to full unambiguous range (nominally 10-15 km). However, atmospheric attenuation and the limited availability of volumetric particulate scatterers in the Rayleigh regime negatively impacted power return and presented significant clear-air (e.g. non-precipitating) return constraints.

Table 2. Comparison of the technical specifications and performance metrics for the DOE-X prototype and the TTUKa radars.

Parameter	Current TTUKa Specifications	Target Prototype Specifications	Performance Metric
TARGET PERFORMANCE ENHANCEMENTS			
1. Data Availability			
1a.Waveguide Loss/Spectral Purity	0.576 dB/m	0.108 dB/m	5.3:1 Improvement
1b. First Stage Down Conversion Mixer Loss	20.4 dB	7.5 dB	2.7:1 Improvement
1c. Low Noise Amplifier Noise Reduction	2.9 dB	1.4 dB	2.1:1 Improvement
1d. Signal Quality Index Improvement	NA	NA	10% increase for all data between 3-15 km in range
2. Real-Time File Conversion	NA	NA	Functional output in NetCDF format in real-time
3. Real-Time Editing	NA	NA	First order editing available in real-time
4. Resolution and Speed			
4a. Range Resolution (Range Gate Spacing)	15 m*	15 m*	Preserved range gate spacing using an equivalant pulse
4b. Azimuth/Elevation Resolution	0.33°	0.50°	Preserve a 0.5° half power beam width shown to be applicable for wind farm complex flow work using the TTUKa radars**
4c. Antenna Scan Speed (Azimuth/Elevation)	30°/6°	30°/6°	Preserve the scan speeds
ADDITIONAL GENERAL SYSTEM COMPARISONS			
Peak Transmit Power	212.5 W	10,000 - 11,000 W	
Transmit Frequency	~35 GHz	~9 GHz	
Wavelength	~8 mm	~3 cm	
Antenna Diameter	1.83 m	4.5 m	
Pulse Length	12.5, 20 μs	12.5, 20 μs	
Pulse Repetition Frequency	up to 15000 Hz	up to 4000 Hz	
Azimuthal (PPI) Resolution	0.352°	0.352°	
Elevation (RHI) Resolution	0.1°	0.1°	

*Based on a 20 μs modulated pulse typically used for wind farm complex flows work

**Applicable value based on initial papers published using measurment acquired with the TTUKa radars. Maximum usable range also indirectly defined through beam spread limitations.

The density of atmospheric scatterers cannot be controlled, but the radar design impacts atmospheric attenuation and the nature of the potential scattering mechanism. RF absorption characteristics are primarily related to how close the given RF frequency of interest is to the resonance frequencies of oxygen, water vapor and liquid water content. Although the oxygen absorption coefficient varies by only a few tenths of a dB/km between Ka and X-bands, the water vapor absorption coefficient at 25% relative humidity is more than 12 times greater for the TTUKa radars than the DOE-X prototype and liquid water absorption is more than 20 times greater with the TTUKa radars than the DOE-X [10]. Hence, the DOE-X wavelength is less susceptible to attenuation and therefore provides more power to the target, and increases the maximum range of coherency for most atmospheric environments.

Within the Rayleigh scattering regime, the received power returned from particulate backscattering is proportional to the particle diameter, up to a diameter of approximately 1/3 of the wavelength of the radar. For the TTUKa radars, this linear power return region is valid for particle sizes up to approximately 0.3cm in diameter and would include dust, pollen and small insects. For the DOE-X, this linear power return region is valid for particle sizes up to approximately 1.1cm in diameter, encompassing a much broader range of available atmospheric particulates and insects.

Rapid gradients in temperature/density can also lead to changes in refractive index, which can result in specular reflections (i.e. Bragg scattering) and backscattered power [11]. This backscatter can contribute to return power in certain atmospheric conditions; specifically during nocturnal periods with large radiational cooling near the ground. The backscattered power is strongest for more vertically pointed radars and longer wavelengths. The scientific literature maintained mixed opinions on whether Bragg scattering would significantly contribute at X-band [12], but the mechanism does contribute to the DOE-X prototype (see later discussion) and fills the measurement volume with a relatively continuous return when available. Given its millimeter wavelength, Bragg scattering did not contribute to the TTUKa's return power in any meaningful way.

Transmitter Technology and Power Improvements

The use of pulse compression requires that the complex, non-linear frequency modulated chirp be mathematically formulated and constructed at the system intermediate frequency (IF) by the digital signal processor, then up-converted to low-power RF by superheterodyne mixing. The low-power RF modulated signal is then amplified by the transmitter. The need to amplify the RF complex modulated signal required to perform pulse compression precludes the use of a simple conventional Magnetron oscillator based transmitter, with the two remaining available choices for consideration being the Klystron and the TWT amplifiers. Based on physical size, available duty cycle, external cooling requirements, A/C line voltage and power requirements, expected lifespan, and overall cost, a coupled-cavity, dual TWT technology was chosen for the DOE-X prototype. This innovative transmitter design has never been implemented previously for the enhancement of meteorological radars.

The DOE-X coupled transmitter consists of two 6 KW, 8% duty cycle, TWT amplifiers which are combined electronically to produce an estimated peak output power of approximately 10.5 KW, while remaining at 8% maximum duty cycle. For a 20 μsec compressed pulse width, the maximum pulse repetition frequency available without exceeding the 8% duty cycle is 4000 Hz. For comparison, the TTUKa TWT amplifier peak power specification is 200 W. In a typical wind plant setting, the TTUKa radars utilize a PRF as high as 15,000 Hz while transmitting a compressed pulse width of 19.1 μsec yielding an average power of 57.3 W. For the DOE-X operating at a comparable 19.1 μsec compressed pulse width yields 626.7 W. Thus, the DOE-X prototype system, while operating under the same sampling conditions of a typical wind plant deployment, will generate more than an order of magnitude more normalized average power density for any given range.

Other Radar Design Enhancements

Waveguide loss was reduced from 0.576 dB/m to a targeted 0.108 dB/m. Waveguide attenuation tables for WR-28 vs. WR-90 coin silver plated copper waveguide indicate a reduction in attenuation per unit length of 5.3:1 contributing to an increase in the spectral purity of both the complex modulated transmit pulse and the received target image of the DOE-X over the existing TTUKa. Although the TTUKa and DOE-X transmitters operate within different frequency bands, the complex modulation envelope of the pulse compression signal is identical. As such, a lumped-parameter comparison of the spectral purity of the received signal from a coincident target (obtained by utilizing identical pulse compression modulation indexes) was made between the two systems to verify the improvement. The first stage down conversion mixer loss was to be reduced from 20.4 dB to a targeted 7.5 dB. This 2.7:1 reduction in signal path loss in the down conversion stage of the receiver is added directly to the dynamic range of the analog receiver chain. The TTUKa loss was directly measured by laboratory standardized equipment, whereas the DOE-X loss target was based originally on the manufacturer's specification of the first down conversion mixer, but later measured during the initial testing and calibration phase of the new receiver design to verify the improvement. The low-noise amplifier noise (LNA) associated loss was to be reduced from 2.9 dB to a targeted 1.4 dB. This additional signal path loss reduction of over 2.1:1 in the LNA is also added directly to the dynamic range of the analog receiver chain as in the first conversion mixer stage. The noise figure for the TTUKa LNA was measured in the laboratory and the DOE-X was originally based on the manufacturer's specification, but later verified during the initial testing and calibration phase of the new receiver design.

Comprehensive Verification

While the identified design changes yield enhanced system sensitivity, and an expectation that data availability will improve in almost all atmospheric conditions for the DOE-X prototype relative to the TTUKa radars, the coupling of these design changes with changes in atmospheric scattering regimes yields a complex system that requires verification. Hence, a comprehensive performance metric was established for the integrated system; specifically, that the signal quality index for the DOE-X must be increased by a targeted 10% relative to the TTUKa radar. The results of the DOE-X/TTUKa comparative testing indicate that the new DOE-X not only meets, but far exceeds, this performance metric. The details of this comparative testing is included in the Functionality and Performance Testing section of this technical report.

Real-Time File Conversion and Editing

Data files in the NetCDF format were to be provided as output from the DOE-X prototype to provide an accepted and user-friendly data format for downstream commercial post-processing and product generation. The TTUKa radars output a complex binary file structure, which is difficult for most industry users to use, so a processing routine was developed to execute this file conversion in real-time. Measurement files collected during the testing period were used to verify the NetCDF data structure was functional, and could easily be incorporated into other software environments through established NetCDF read functionality (e.g. Matlab).

First-order quality assurance/quality control (QA/QC) was also implemented in the real-time data stream, and this change effectively enhanced post-processing development efficiency as the basic editing was already completed. Real-time QA/QC includes data thresholding to remove data known to be associated with fixed targets, noise, and other erroneous returns. This thresholding process removes data bins from all radar moments associated with data values that known to be outside of the bounds of common meteorology (e.g. very high return powers associated with a point targets, very low signal quality indices associated with noise, etc.). In addition to data thresholding, sector scan "jitter" removal is also conducted. Jitter occurs on every other sector scan and represents an erroneous azimuthal offset that is caused by antenna dynamics (hysteresis) as it transitions from one sector to the next. This jitter offset is nominally a known, constant value that can be accounted for in the real-time QA/QC processing of the azimuthal information of the data. A configuration file exists so that a user can tune the data thresholding parameters and jitter offset value, as appropriate. The TTUKa radars do not provide this automated data editing process, and do not have an onboard server to execute this functionality, so the QA/QC'd NetCDF data files from the testing period were used to verify the real-time editing process is functional and provided a comparison to the original data set (i.e. without editing).

Spatial and Temporal Resolution

The preservation of spatial and temporal measurement resolution were required to provide relevant wind plant complex flow measurements over a large experimental domain. An along beam range resolution of 15 m was required, which ensured that wind plant complex flow features, including detailed turbine wake structure, could be adequately represented as proven by the existing TTUKa radars [4, 5, and 6]. Range resolution is purely a function of the pulse width (conventional mode), or formulation of the complex, non-linear frequency modulated chirp (pulse compression) and digital signal processor. The engineering effort that was invested into advancing the compressed pulse for the existing TTUKa systems was directly transferrable to the new DOE-X prototype, and thus, the exceptional radial resolution was retained at 9m for the 12.5 μsec and 15m for the 20 μsec compressed pulses. Data files were used to verify range gate spacing.

Azimuth/elevation resolution and oversampling capabilities were also to be preserved. Specifically, a 0.5° beam width was required. This beam width, coupled with the 0.352° horizontal and 0.1° vertical oversampling available via the radar control software, has been proven by the existing TTUKa radars to adequately resolve wind plant complex flow features, including detailed turbine wake structure, over a large wind plant. Azimuthal (i.e. across-beam) resolution of a radar system is generally expressed in terms of the parabolic reflector 3 dB beam width and decreases as a function of range due to beam spread (horizontal and vertical dimensions). Azimuthal beam width is inversely proportional to reflector diameter as well as parabolic reflector gain. With a desire to maintain gain, while limiting the overall reflector diameter to a manageable and commercially available size, the new DOE-X prototype supported a 4.5 m parabolic antenna with 3 dB beam width of 0.49°. The corresponding reflector gain was 52.9 dBi.

Temporal resolution (i.e. revisit intervals) is also an important factor for applying the technology to document wind plant complex flows. TTUKa antenna scan speeds (i.e. a horizontal antenna scan speed of 30° s^{-1} and vertical antenna scan speed of 6° s^{-1}) were required. The volume completion times of measurement files and detailed logs of antenna motions were used to verify that the scanning speeds were preserved relative to the TTUKa radars.

Portability and Semi-Autonomous Operation

The existing TTUKa systems are mobile and can be rapidly deployed and in operation in a matter of minutes upon arrival to a site. The command and control system for the DOE-X prototype was designed to be globally transportable within a standard 8' W x 8.5' H x 20' L sea-container. The antenna, pedestal and radome subsystems were designed to be temporarily packed into a standard 8' W x 8.5' H x 40' L transport sea-container. Within a week's time, the entire system can be easily assembled with assistance of a small truck crane and a three-person installation crew. System startup, major subsystem status reporting, radar task configuration, radar task scheduling, a real-time radar display and system shutdown capabilities can be made available via a secure remote network control user interface, but no communications are currently included in the existing DOE-X prototype. Once the DOE-X system is assembled, the system can continuously operate unmanned throughout the duration of a given deployment.

Major Component Layout and Descriptions

All DOE-X system electronics (including the transmitter, receiver, digital signal processor, and data storage hardware) were housed inside a 20' double door sea container and powered by a 15KVA, 3-phase, 60Hz, four wire plus earth ground, 208 volt line-to-line inlet supply that was readily available at the NWI field site location. However, the system can reconfigured to accept common US (60Hz) and European (50Hz) 3-phase inlet power sources. The pedestal, antenna, and radome were placed above the sea container atop an exoskeleton support structure, which straddles the sea container. The sea container and exoskeleton were bolted to concrete footings installed onsite. A schematic of the DOE-X radar deployment is provided in Figures 5 and 6, while a picture of the actual deployment is provided in Figure 6.

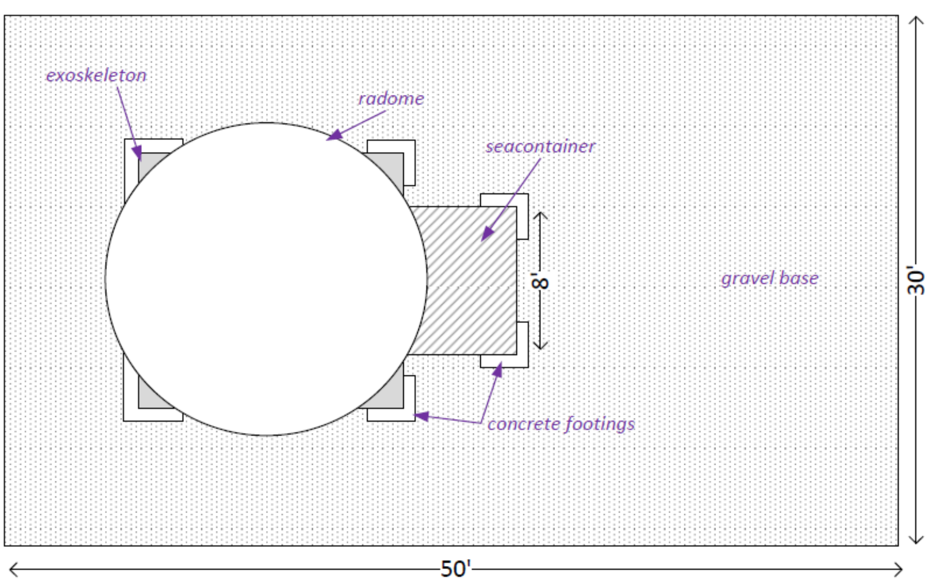

Figure 4. Conceptual plan view of the DOE-X prototype radar site at the NWI Reese Technology Field Site.

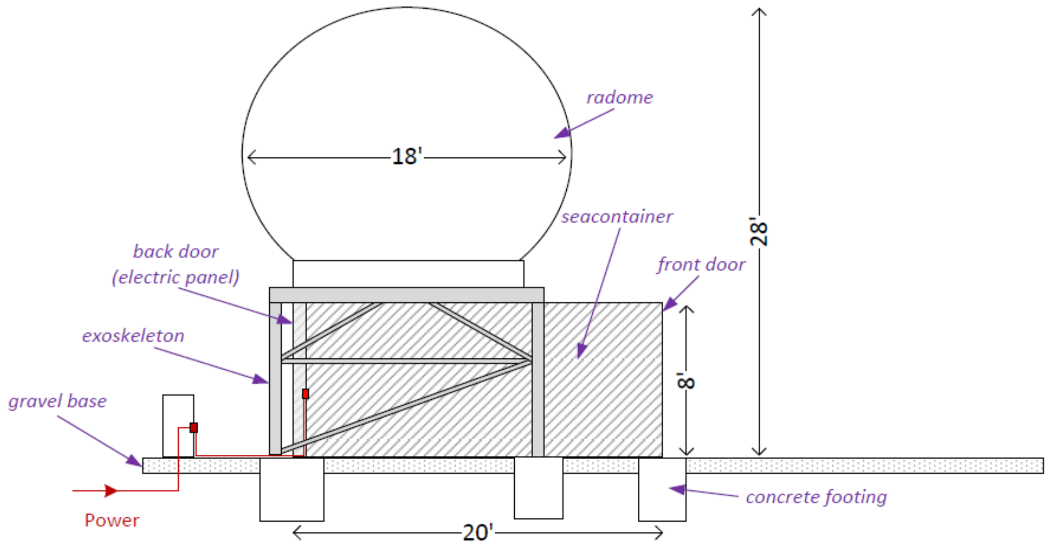

Figure 5. Conceptual elevation view of the DOE-X prototype radar site at the NWI Reese Technology Field Site.

A brief description of the major radar subsystem components follows:

a. **Pedestal and Antenna Subsystem**: The radar pedestal is the hardware component responsible for the mechanical rotation of the antenna. The antenna assembly, which consists of the parabolic reflector, feedhorn support struts and associated single-polarization feed horn, is responsible for focusing all transmitted and received radiation. For the DOE-X system, the pedestal and antenna were supplied as an integrated system, but had to be modified for use at X-band.
b. **Signal Processor:** After down conversion to the baseband IF frequency of 60MHz through the dual-conversion receiver chain, the digital signal processor provides the real-time processing of all incoming radiation into raw data files, and is also responsible for driving the system operation.
c. **Transmitter:** The transmitter is responsible for generating the emitted microwave signal. In order to maximize the peak output power while maintaining stringent pulse-compression modulation capabilities, an innovative dual-coupled cavity, fully coherent, travelling wave tube amplifier was utilized.
d. **Radome:** The radome is a finely tuned protective cover for the DOE-X antenna and pedestal to mitigate the impacts of weather, wind loading, and objects striking the antenna.
e. **Duplexer (Circulator):** The duplexer provides isolation between the transmitter and the receiver and is a ferromagnetic device that alternates connecting the antenna to the transmitter and then to the input of the receiver chain during a transmit/receive cycle via Faraday rotation.
f. **Receiver Protector:** The receiver protector is a passive, self-triggering, radioisotope primed, high-speed gas discharge tube that further shields the input of the receiver chain from any spurious high-energy output from the duplexer.
g. **Azimuth Rotary Joint:** The azimuth rotary joint is a complex waveguide joint that allows transmitted and received radiation to pass through the horizontally rotating antenna pedestal.

The azimuth rotary joint requires an integrated slip ring package in order to commute power and command and control signals to the pedestal unit.

h. **Receiver Chain Components:** The receiver chain is responsible for the down-conversion of the X-band signal received by the radar to the 60MHz intermediate frequency input into the digital signal processor, as well as the up-conversion of the 60MHz complex pulse-compression modulation from the digital signal processor for input into the traveling wave tube amplifier. The receiver chain is comprised of a series of RF components including precision local oscillators, mixers, splitters, isolators, filters and amplifiers.

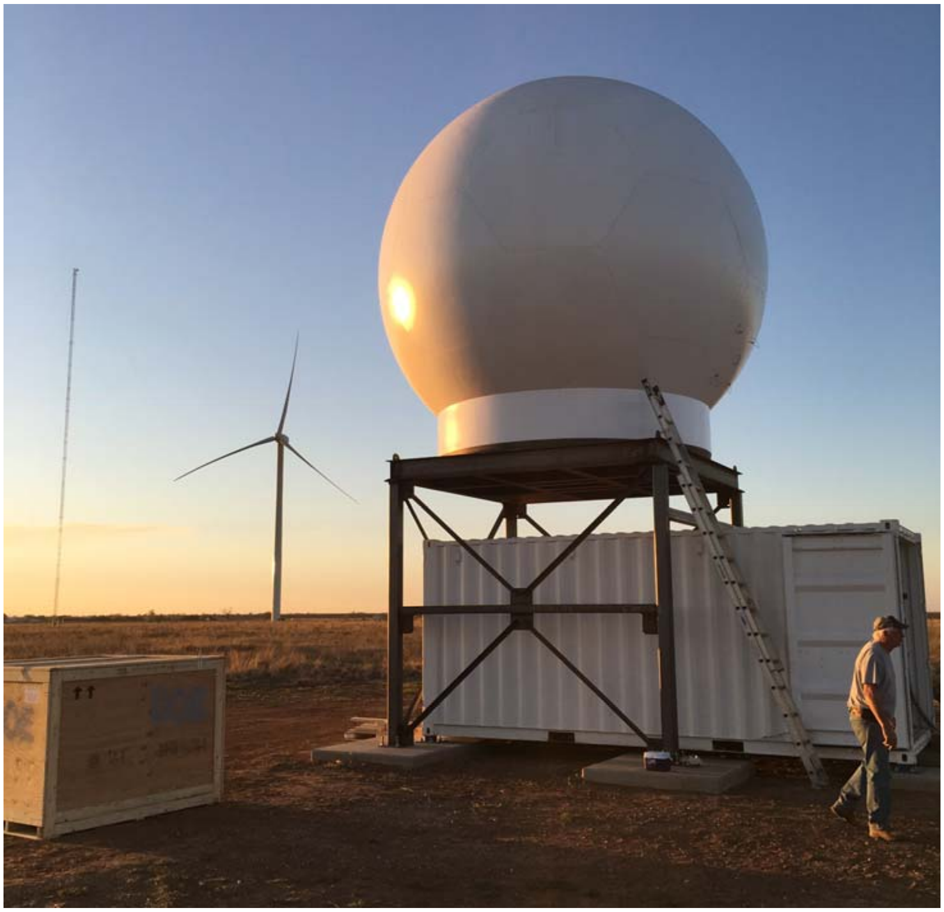

Figure 6. Photograph of actual DOE-X installation at the NWI Reese Technology Field Site.

Integration and Installation Process

The components of the DOE-X radar were developed by a variety of suppliers across the world. The transmitter and receiver chains were integrated by the project team and tested at the supplier's laboratory (Figure 7) prior to shipment. During this step, performance testing for the transmitter was verified, documented via test reports, and then distributed to DOE. Other components (e.g. antenna) were tested and verified by the supplier, independent of the project team. Test reports were then provided to DOE. Once the major subcomponents arrived at the NWI facility in Lubbock, additional integration, assembly, and modification efforts commenced.

Given that this was a prototype system, large subcomponents of the system were integrated in the warehouse area of Building 250 for further modification and verification prior to final installation in the field. The pedestal/antenna subsystem had to be modified for use at X-band and was assembled (Figure 8) using a forklift. The custom azimuth and elevation rotary joints were then installed (Figure 9), followed by the waveguide support struts and feedhorn (Figure 10). Additional waveguide support brackets were designed and fabricated at a local machine shop. Given the custom nature of the DOE-X prototype, initial straight-run waveguide measurements were made, procured and fitted, then final complex-bend waveguide measurements were made, and the last pieces of waveguide procured and fitted.

At the same time, the radome subsystem was assembled in three large sections (Figure 11). The base section consisted of the riser and base panels, while the upper portion of the radome, made of pentagon and hexagon panels, was assembled in two sections and then merged. This assembly was required for several reasons. First, the riser panels needed to be fitted to the mounting plate of the exoskeleton support platform. Second, measurements of the radome and antenna were required to develop an appropriate technique for the final field assembly. Finally, the team needed to gain experience assembling the system prior to the field integration.

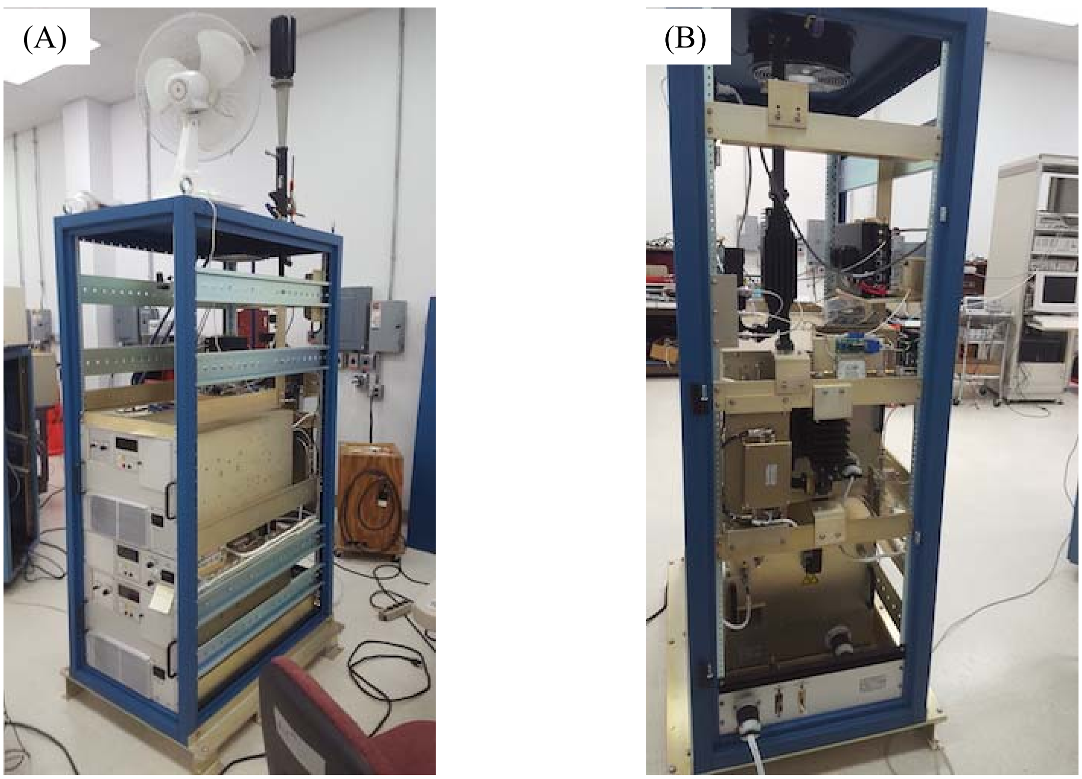

Figure 7. Side and front (A) and back (B) views of transmitter rack at supplier during final configuration and acceptance testing efforts. Rack sidewalls have been removed to show internal detail.

The project staff designed and fabricated the exoskeleton support structure (Figure 12). The pedestal mounting plate, custom fabricated from a 1” thick, 4’ W x 4’ L steel plate with a water jet cutter, and the support platform were the first components assembled. The radome riser was then lifted on the support platform and the mounting holes were drilled in place. The radome riser was then removed and the support platform was rotated. The legs and cross bracing were then assembled. Once the entire structure was assembled, it was moved as one unit.

While radar integration work was ongoing in the warehouse, the command and control sea-container was delivered to NWI Building #250 and stored outside. When the container arrived, it had been reinforced by the supplier per the design and guidance of the project staff to support the mounting of the electrical infrastructure. Upon arrival, the walls were insulated and covered with plywood, the floor was coated with an industrial epoxy finish and the walls were painted. The HVAC unit, lighting, and all electrical distribution boxes were then installed, and the unit was prepared to accept the transmitter and radar processing server racks. Additional work also occurred at the site as it was prepared to accept the radar. Site preparations, completed by local contractors, included installation of concrete footings and providing power service.

Figure 8. Antenna/pedestal subsystem assembled in the warehouse area of NWI's building #250.

After the integration of the major DOE-X subcomponents at the NWI warehouse was complete and the site prepared, the system was ready for final installation, which was broken into three main phases. During the first phase, the command and control sea container and exoskeleton platform were moved to the site and anchored to the concrete footings (Figure 13). This phase occurred in just a few hours.

A second, more intensive phase of the installation followed on a subsequent day when an appropriate weather window was identified. During this phase the antenna, pedestal, and lower radome sections were loaded and transported to the site. The pedestal was first unloaded, followed by the antenna. The two systems were then mounted together at ground level, and the feedhorn, struts, and waveguide were re-attached. The lower radome section was also attached to the exoskeleton support ring. Following these preparatory steps, the entire pedestal/antenna subsystem was then lifted and attached to the exoskeleton mounting platform in the center of the lower radome section. Subsequently, the upper portion of the radome was moved from the warehouse to the field site using a man lift. This step was completed by walking the section to the site (Figure 14). Once on site, the upper portion of the radome was lifted into place to cover the antenna/pedestal subsystem (Figure 15), and mounted to the lower portion.

Figure 9. Azimuthal (A) and elevation (B) rotary joints installed on the antenna/pedestal subsystem.

Figure 10. Struts and feedhorn installation on the front side of the antenna. Waveguide and supporting brackets were installed down the strut.

Figure 11. Radome subsystem construction.

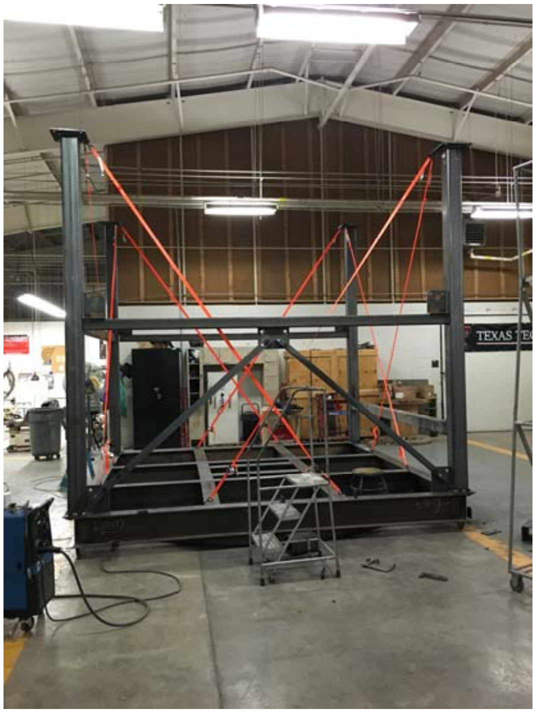

Figure 12. Exoskeleton support platform.

Figure 13. Phase one of the radar prototype installation at the site, as the sea container and exoskeleton platforms are mounted to the foundation.

The third phase of the installation did not include any lifts, and could be completed regardless of the weather conditions. During this phase, the racks were placed and mounted to the floor inside the command and control sea container, the bellows connecting the bottom of the exoskeleton platform and the top of the command and control sea container was installed, all cabling and waveguide runs between the pedestal and command and control racks were completed, and power was connected to the container.

Figure 14. Upper section of radome being moved to the site.

Figure 15. Upper portion of the radome being lifted into place.

Site Characteristics

The DOE-X was deployed for initial testing and data collection at 33.613° N/102.048° W which is close to the northern property line of the NWI field site. This site was chosen to avoid influencing the wind flow into the Scaled Wind Farm Technology (SWiFT) facility or TTU 200 m tower form the climatologically preferred southern wind direction. This location is approximately 340 m northeast of the 200 m instrumented tower, and 380 m north northeast of the SWiFT control building (Figure 16). The test site is characterized as flat and open in every direction, except for the existing low level structures, meteorological towers, and the research and utility scale turbines in the area. The closest residence is located approximately 1.2 km from the site, and there are no known issues with respect to wetlands, historic sites, flood plains, etc. A NEPA review was conducted prior to construction. The westernmost runway (shown in Figure 16) associated with the former Air Force Base has been closed for usage, while the eastern runways (not shown) only provide limited access to private aircraft. The maximum height of the DOE-X deployment (peak height of the protective radome) is approximately 28 feet above ground level.

Figure 16. Google Earth provided imagery of the DOE-X installation location.

Validation and Testing

Functional Testing

Following the installation process, functional testing was initiated. The UPS and power distribution was verified, the computer and transmitter racks were energized and their functionality verified, and the pedestal/antenna was verified for both azimuthal and elevation control. During this time period, various changes to the radar operations and control software were implemented and tested for the first time, as demanded by the custom nature of the radar.

During early testing of the system, the coupled transmitter was operated at a low PRF in conventional mode to gently initiate the testing process for the coupled transmitter. As the system was stepped towards an operational state, the operations and control software were further modified, and the operation of the radar system was slowly advanced to reach a semi-autonomous state. Initially, manually triggered surveillance (full 360°) scans provided the first measurements, but these scans were quickly replaced by scheduled surveillance scans executed every 15 minutes automatically executed without user intervention. Plan Position Indicator (PPI) sector scans were then tested in a similar manner, followed by Range Height Indicator (RHI) scans. Each of these efforts succeeded, but not without some additional effort to troubleshoot command and control issues related to the waveguide dehydrator.

The pace of the scan execution was then increased to almost continuous, instead of once every 15 minutes. During this accelerated testing, the antenna dynamics were questioned, as scan times did not match those previously anticipated from the TTUKa radars. Additionally, some volumes were incomplete (e.g. only yielding a few scans relative to the total number of scans expected). These issues have since been solved through repeated interaction with the supplier. Additionally, azimuthal scan-to-scan angles lacked repeatable, but this issue was later resolved through the installation of an additional custom designed waveguide support bracket adjacent to the azimuthal rotary joint.

Performance Testing

Initial qualitative performance comparisons between the DOE-X and TTUKa radars were completed based on limited data (as seen in Figure 17) collected over a few days of operations.

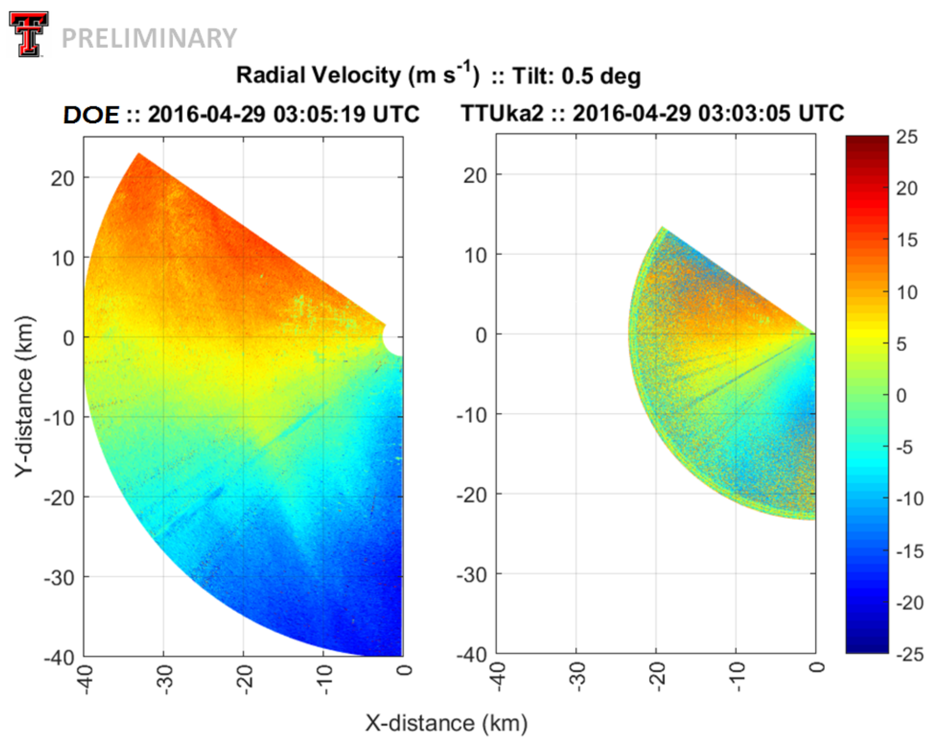

Figure 17. Comparison of data from DOE-X (left) and TTUKa radar (right) systems from the same non precipitating “clear air” environment.

The qualitative assessment yielded the following results:

- On the first assessed “clear air” day (i.e. without precipitation), the DOE-X would have provided relevant measurements to a range of 15 km approximately 85% of the time. Relative to the historical experience with the TTUKa radars, this represented a monumental step forward.
- As expected, limited comparisons obtained using the radar systems in precipitating atmospheres resulted in the DOE-X maintaining more data availability at distant ranges.
- The DOE-X provided an enhanced range potential by using a lower pulse repetition frequency (which still yields equivalent or better data availability relative to the TTUKa).
- The DOE-X prototype effectively benefited from Bragg scattering during the nocturnal hours, while the TTUKa did not. This result represents a significant advance that allows for relevant radar operation during nocturnal hours in some warm season atmospheric conditions.
- The severity of radar artifacts (in particular, multiple trip echoes where power returned from a given transmitted pulse is not received until the transmission of one or more additional pulses) increased with the DOE-X prototype relative to the TTUKa radars. The result is likely a function of the vast increase in power of the DOE-X relative to the TTUKa radars. Similar to the TTUKa radars, ground clutter and turbine induced artifacts are also exacerbated by using pulse compression, relative to a conventional pulse.

Based on the initial qualitative data, the project team was satisfied that it had achieved all its objectives, but a more thorough quantitative examination remained. Through the examination of the initial measurements, additional configuration changes and validation checks were provided with time. For instance, the pedestal was re-leveled to account for settling of the foundation which was noticeable in the low elevation scans. After the system had reached a stable performance state, quantitative performance testing relative to the TTUKa radar was initiated. During this short period, a TTUKa radar was co-located with the DOE-X as shown in Figure 18.

Figure 18. Co-located DOE-X and TTUKa radar positioned for performance testing.

Given a trimmed testing budget due to DOE budget restrictions, and the unknowns associated with clear air capability in uncooperative atmospheres (i.e. low Rayleigh scattering regimes), a challenging environment on 3-4 August 2016 was chosen for the quantitative performance evaluation. After all, evaluating the new DOE-X prototype's capability in the most difficult environments, relative to the TTUKa radars, was the most important objective of the project. For this quantitative evaluation, the DOE-X and TTUKa radars both scanned 90° PPI sector scans in the same direction using a scan speed of 30°/sec. This process was repeated every 15 minutes for a 24 hour period using an elevation angle of 1°. Both systems employed a 20 µsec compressed pulse. The DOE-X and TTUKa radars employed pulse repetition frequencies of 4,000 and 12,000 Hz, respectively, which yielded maximum ranges of 34.5 ad 9.5 km, respectively. The collected measurements were then used for the analysis.

Since the maximum range for the DOE-X and TTUKa radar systems differ, two sets of statistics were generated. The first set of statistics was calculated over the common ranges of 3-9.5 km. To assess baseline data availability, data associated with a signal quality index (SQI) of less than 0.2 were removed; this threshold has been traditionally used in some of the wind plant complex flows research using the TTUKa radars to remove noisy data. Next, the number of remaining data bins (with SQI>0.2) from each scan was counted and a percentage relative to the maximum number of data bins possible was calculated at each range. These percentages were then compared, and the difference calculated.

Over the 24-hour period, the DOE-X averaged 35.8% more data availability than the TTUKa radar across the common ranges from 3-9.5 km relative to the maximum amount possible. As shown in Figure 19, the maximum data availability by the TTUKa never achieves 20% even at minimal ranges (e.g. 4 km), while the DOE-X reaches a maximum value near 70% just after sunset and only dips below 20% for brief periods. Fluctuations during the 24-hour period highlight the different scattering regimes that occur, as Rayleigh scattering due to elevated particulate is maximized during the day time. During the evening, the elevated particulate material "falls out" of the atmosphere as thermal mixing subsides, which leads to a decrease in data availability from 0-2 UTC. However, for the DOE-X radar, a rapid increase in data availability occurs in the early overnight hours (2-3 UTC) as a Bragg scattering regime becomes entrenched. This impact cannot be seen in the data availability for the TTUKa radar due to its inherent limitation to benefit from Bragg scattering with a shorter wavelength.

The target performance metric related to data availability that was proposed for the project (Table 2) was focused on increasing the SQI by 10% for the DOE-X relative to the TTUKa radar. The SQI moment provides a normalized reference to the signal-to-noise ratio for each radar data bin with values ranging from 0 (noise) to 1 (high quality data); higher values correspond to higher data availability. The SQI moment was compared for all bins between the common ranges of 3-9.5 km. In this case, the raw measurements were edited to remove where the total power > 0 dBZ (resulting from point targets/ground clutter) and/or the spectrum width was greater than 2.7 m/s (indicative of noise). Averaging across the entire time period, Figure 20 provides the mean SQI value of both systems by range, with the DOE-X resulting in a significant increase at all common ranges, with an average value of 0.46 relative to the TTUKa value of

0.03. This increase represents a 43% improvement relative to the maximum value of 1. It is interesting to note the DOE-X average SQI value only dips below 0.2 at ranges beyond ~19 km.

The powerful advantage of additional data availability from the DOE-X prototype has been highlighted over the common ranges of 3-9.5 km, but by itself this underestimates the true difference between the systems. The DOE-X prototype offers more data availability at the common ranges, but it also provides additional data out to its maximum range of 35 km (based on a PRF of 4,000 Hz) that is not available with the TTUKa. If these additional data are considered, the improvement of the DOE-X radar is further highlighted. After quality controlling the raw data using a 0.2 SQI threshold, and based on all available ranges on each system, the number of data bins acquired for the entire 24 hour period was counted. The DOE-X prototype radar provides a 5,560% increase in data availability relative to the TTUKa radar. It should be noted that even when the TTUKa data availability is 100%, the DOE-X radar would be expected to produce 3.5 times the amount of data since its nominal maximum range is 3.5 times that of the TTUKa radar.

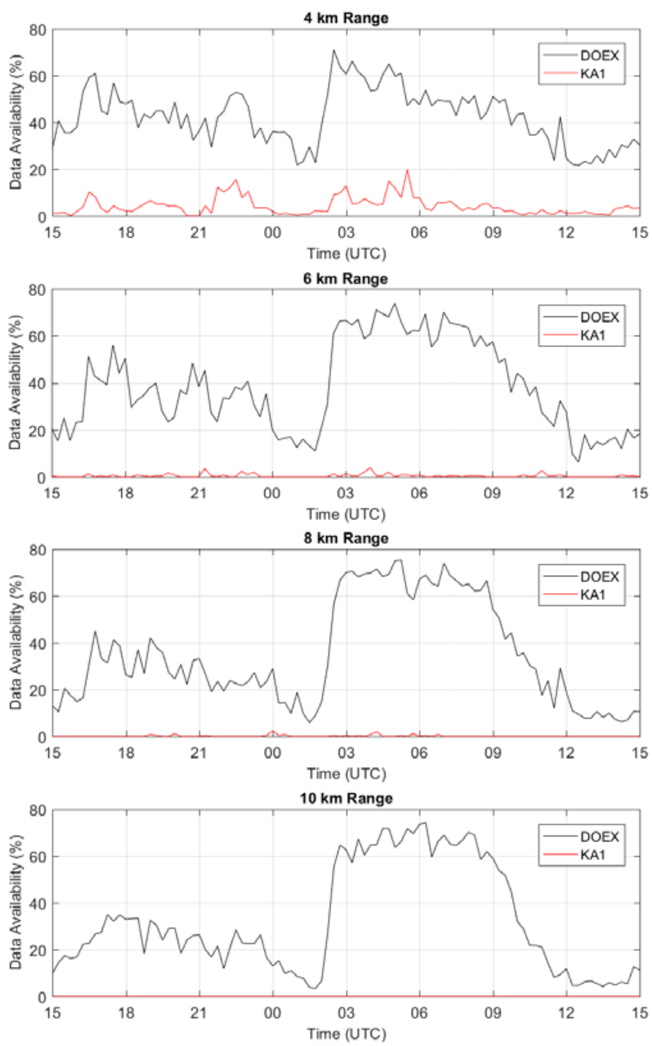

Figure 19. Comparison of DOE-X and TTUKa data availability over a 24-hour period on 3-4 August, 2016.

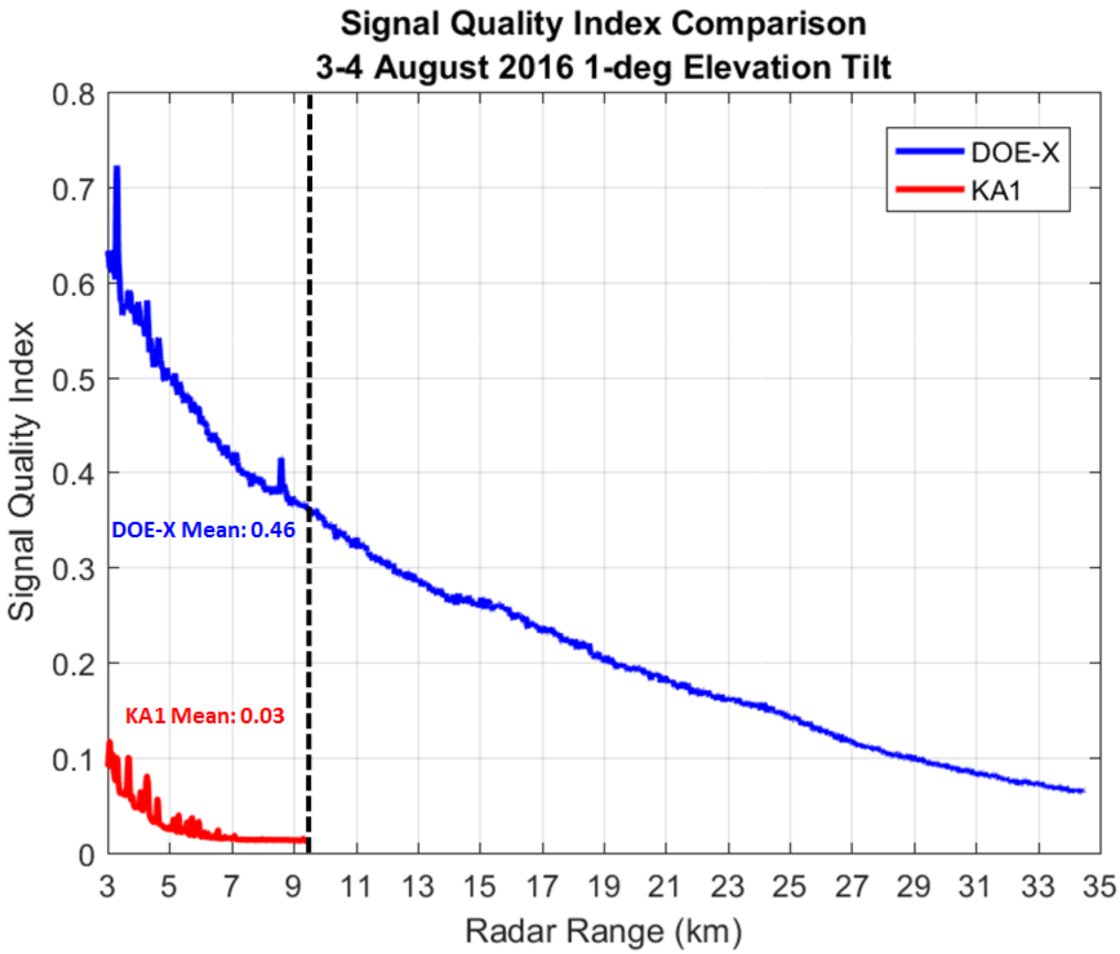

Figure 20. Plot of mean SQI by range from the entire 24-hour test period for both the TTUKa and DOE-X prototype radars. Note the range axis starts at 3 km.

While a detailed long term study of data availability was beyond the scope of this project, qualitative assessments can be made regarding the performance of the DOE-X prototype based on the intermittent DOE-X measurements that have been collected since its installation. Given the seemingly well correlated level of coherency for the DOE-X relative to the performance of the national NEXRAD radar system employed by the National Weather Service, the NEXRAD's performance throughout a year can be used as an indicator. Hence, performance during the spring, summer and fall, will likely be better than performance in the winter. The warm season is marked by increases in both Rayleigh and Bragg scattering regimes, which means that during portions of the warm season (spring and fall in particular), data availability through 15-20 km will likely top out at 85-90% for multiday day periods, and carry a significant average ~50-70% over longer periods. During the middle of the summer, the performance is likely to drop as Bragg scattering seemingly becomes more limited, while, during the winter the current technology would drop farther as both Rayleigh and Bragg scattering is significantly reduced. Note, while the NEXRAD is a wonderful radar for weather detection, it is a very large system and does not nominally provide details regarding wind plant complex flows.

Wind Energy Relevant Measurement Examples

While not the focus of this award, the initial measurements made in support of this project offered interesting insights of relevance to the wind energy industry. As an example, a 24-hour period of data was employed to compare with the stability measurements from the nearby TTU 200 m tower. As illustrated in Figure 21 (top), the acquired DOE-X measurements provide dramatic examples of rapidly changing boundary layer wind flow structure as revealed by the acquired radial velocity fields. At 22 UTC, during the afternoon and with an unstable convective boundary layer in place, "cell like" structures translate in the radial velocity field. However, during the evening transition these structures are quickly replaced with a laminar structure that is associated with the stable nocturnal boundary layer. An example of this structure is provided for 8 UTC, where both wind speed shear and wind direction veer are present. Then shortly after sunrise (15 UTC), the boundary transitions back towards unstable, but for a brief period near mid-morning, when it remains neutral to slightly unstable. During this time period, the wind flow structure is dominated by streaks seen in the radial velocity field. The varied boundary layer structures (as observed over the course of a diurnal cycle) would all impact a wind plant differently, with the featureless nocturnal flow field providing minimal background turbulence to disrupt and mitigate turbine wakes, and perhaps offering the best target for proactive wind plant level controls activity.

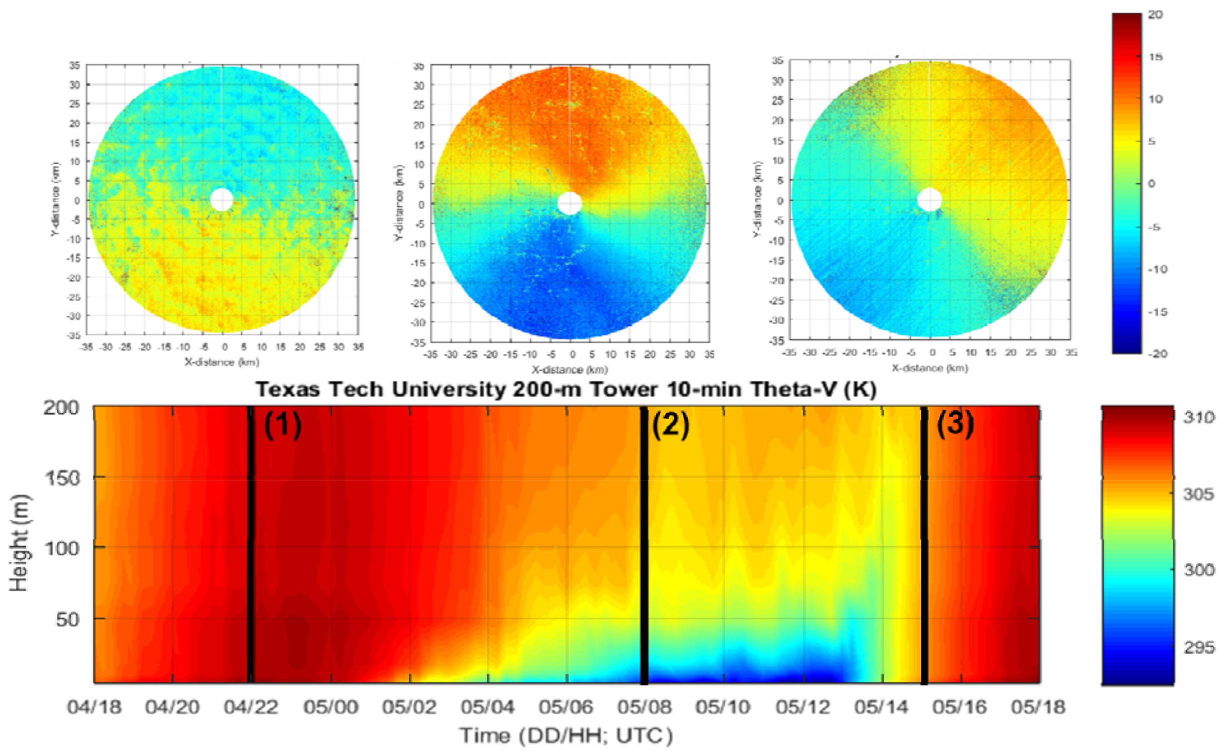

Figure 21. Radial velocity (m/s) acquired from 360° surveillance scans acquired at 22 UTC (top-left), 08 UTC (top-middle), and 15 UTC (top-right) using the DOE-X prototype, and a time history of virtual potential temperature (K) profiles from the nearby TTU 200m tower (bottom), where the time of each radar scan is noted.

Based on unrelated interests, acquired DOE-X radar measurements have also been thresholded using a different technique to document if the technology could identify and track bird traffic. This effort was successful, and bird traffic could be separated from the background flow field. Figure 22 shows a raw unfiltered radial velocity sector scan acquired from a non-precipitating environment that highlights a variety of birds embedded in the background flow field. The individual birds can be followed scan-to-scan (i.e. in time), if they stay within the radar volume. The birds are also evident in other radar moments (i.e. power and spectrum width), which have been excluded for brevity. This discovery opens the door for using the DOE-X radar systems for multi-purpose deployments looking to learn about wind plant complex flows, but also track avian activity. It should be noted that the avian tracking capability is not impacted when the atmosphere is not conducive for measuring the flow field, but would be impacted during periods of heavier precipitation. This application also highlights the benefits afforded by the fast scan speeds/data revisit times, and enhanced spatial data resolution of the DOE-X prototype system.

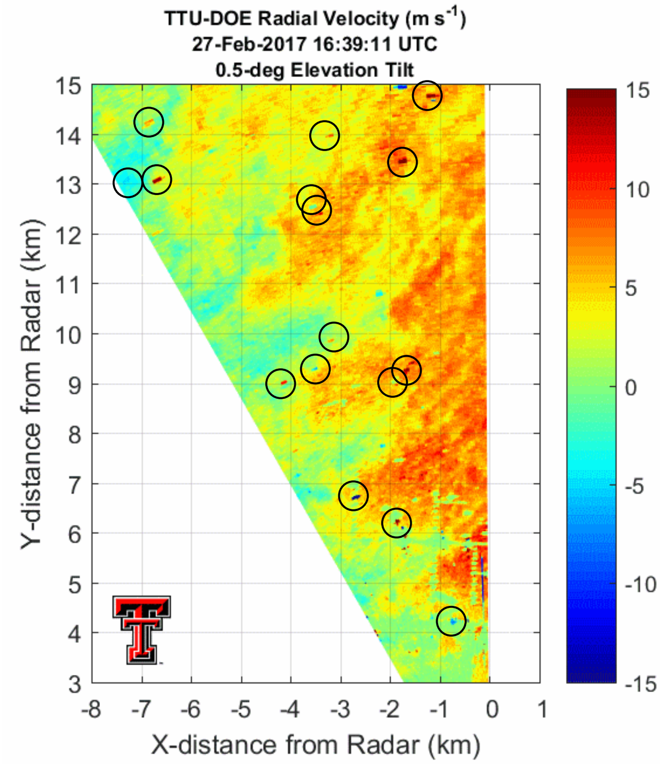

Figure 22. Radial velocity (m/s) field from a sector scan of the DOE-X radar with bird traffic highlighted (i.e. circled).

Related Developments

Outside of the scope of work for this DOE award and through commercial based activities at SmartWind Technologies, more sophisticated processing and post-processing techniques to mitigate radar induced artifacts have been developed. In particular, multiple trip returns/artifacts (e.g. from precipitation located beyond the maximum range) have been shown to be much more substantial using the DOE-X prototype and early stage commercial units (relative to the TTUKa radars). This resulted in a negative influence on the resultant data. To alleviate this concern, phase encoding on the transmitted pulse was employed and resulted in a significant decrease in multi-trip influence. Additional post-processing was also successfully developed for the commercial units to mitigate remaining multi-trip influences, wind turbine induced artifacts, and sea clutter. While sea clutter certainly does not impact the current installation of the DOE-X prototype in West Texas, it would adversely impact offshore oriented measurement campaigns (such as that occurring for DONG Energy off the coast of the United Kingdom).

One industry need that became quickly apparent was to need to develop software tools to visualize, explore, and extract relevant measurements. Even in the simplest of forms, the acquired information from a radar system is substantial in size and can be difficult to explore for untrained individuals. So, SmartWind Technologies developed a user interface (Figure 23) to query relevant information from a measurement archive based on wind speed, direction, time, date and/or data quality. Once the query results are known, the user can explore 10-minute composited or individual radar volumes through the examination of constant height maps, vertical cross-sections and/or profiles. Data can also be extracted to merge with external data sets such as SCADA data. This tool was required by industry, because if untrained individuals are unable to efficiently interact with the measurements, they will never be leveraged to their full potential.

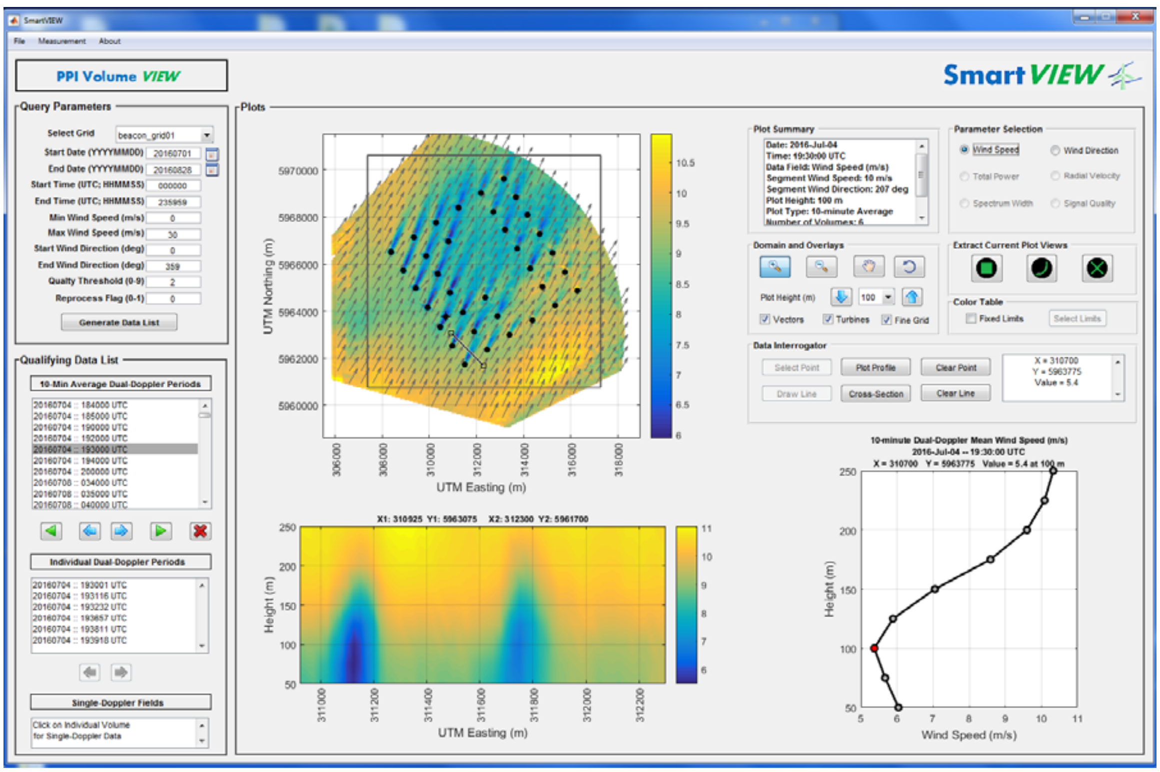

Figure 23. Screenshot of the SmartVIEW application developed by SmartWind Technologies. Data is provided courtesy of DONG Energy.

ACCOMPLISHMENTS

This DOE funded project successfully developed a new DOE-X radar prototype dedicated to advancing wind plant complex flow measurements, and installed it successfully without incident at the NWI field site at Reese Center in April 2016. The development project was completed on budget and on time, with the exception of a small no-cost extension provided to allow more time for additional testing purposes (as requested by the project team). The TRL for the technology was changed from a three to a seven, as the prototype was installed at Reese Technology Center and provided data from the atmosphere.

The DOE-X prototype met or exceeded all performance metrics established in the proposal submitted to DOE. Most importantly, the primary objective to enhance data availability relative to the TTUKa radars was successful, while preserving spatial and temporal resolutions that are conducive for dual-Doppler synthesis of wind plant complex flows. Bragg scattering was identified as a source of additional data availability for the DOE-X prototype; this scattering mechanism was not available to the TTUKa systems due to their wavelength. This addition significantly enhances data availability during the nocturnal period throughout a significant portion of the warm season. The DOE-X prototype has also shown an initial capability to track individual bird activity. While algorithms and approaches are completely undefined at the moment, individual bird traffic is easily identified in the resultant data fields and can be tracked in time (i.e. scan to scan) translating through the region.

Commercial applications of the developed X-band radar concept have started with the deployment of two early stage commercial units for DONG Energy in the United Kingdom by SmartWind Technologies. These units are providing continuous dual-Doppler coverage of the Westermost Rough wind plant. The commercial effort has also resulted in additional software development to assist end users in evaluating, visualizing, querying and extracting relevant radar data from a large archive of measurement. Validation of the commercial units is just starting, but given success, the TRL will be advanced to a level of 8 or 9 through the commercial project.

OUTREACH AND DISSEMENATION

The results of this project are being disseminated using multiple methods. The first public presentation of measurements acquired with the new DOE-X prototype radar was made at the August 2016 Sandia Laboratories Blade Workshop in Albuquerque. Additionally, an in-house seminar was given to the broader TTU community on 1 February 2017. Presentations (and tours) have also been given to a significant number of private entities, which have shown interest in the application of the DOE-X radar technology to wind energy sector. The project team also participated in DOE's peer review process in February 2017, which included the submission of a short summary report and presentation. Finally, the commercialization activity and installation of the early stage commercial units have garnered significant attention via several press releases (e.g. http://www.dongenergy.com/en/media/newsroom/news/articles/first-data-BEACon-radar). Additional presentations, including measurements from the commercial units, are planned for various technical conferences during the remainder of 2017.

CONCLUSIONS

This project has resulted in the development of a radar prototype (TRL of 7) specifically designed to serve the wind energy industry through the measurement of wind plant complex flows. Relative to the benchmark TTUKa radars, the new prototype maintains an enhanced Rayleigh scattering regime, more power to the target, and a significant reduction in return signal loss within the receiver chain. The new technology also maintains advantages over other commercially available technologies with respect to range resolution, maximum range and scan speeds. These advantages are important for conducting synthesis techniques where information from multiple look angles are combined into a single analysis documenting scales of motion relevant for wind energy applications.

The new prototype was installed at the NWI field site at Reese Technology Center in Lubbock Texas. After installation, functional and performance testing was completed. The testing revealed that the project met all of the proposed performance metrics, including the enhancement of data availability and quality relative to the TTUKa radar technology. Specifically, the new DOE-X prototype increased the signal quality index by an average of 43% relative to the TTUKa radar technology, while producing 3.5 to 50 times the amount of data acquired by the TTUKa radar technology. This significant advancement was achieved while preserving the required spatial and temporal resolution for dual-Doppler synthesis for wind farm complex flows. While a comprehensive (e.g. year long duration) study on data availability was beyond the scope of this project, the DOE-X performance appears to be well correlated with respect to the nearby NEXRAD radar provided by the National Weather Service for weather detection, which leads to rather optimistic performance estimates for the warm season period of March to November. The inclusion of Bragg scattering (not possible with the TTUKa radar technology) as a mechanism providing data availability also opens up the nocturnal period for potential operations in supporting atmospheric conditions. This change alone is significant.

The developed prototype provides a basis for continued commercial development. In parallel with this DOE project, two early stage commercial units were deployed by SmartWind Technologies. During the commercial project, additional advancements were made with respect to data reprocessing, and visualization. A full scale validation effort will soon be started using the commercial units, and if successful the TRL will reach an 8 or 9 by the end of the campaign.

The developed technology appears uniquely qualified to significantly contribute to the wind industry and DOE's A2e initiative with wind plant complex flow measurements, highlighting turbine-to-turbine interaction. However, it will also provide plant-to-plant interference measurements across broader regions. These measurements will collectively inform numerical modeling efforts and validate wind plant proactive control techniques. At the same time, while the methodologies are not currently well developed, the new radar technology also appears well suited to track avian traffic, and will likely be able to serve multiple user groups/interests. This outcome will only further enhance the value of the technology.

RECCOMENDATIONS

The DOE-X radar system is available and ready to serve the wind energy industry. While it remains at the NWI's field site, it will be used for continued testing, and supporting various research agendas (including the potential development of more sophisticated bird tracking algorithms). However, it is the desire of TTU to explore a potential move of the DOE-X prototype to an operational wind plant in the United States. Should an opportunity become available, the system will be moved to provide long-term (i.e. multi-year) coverage of wind plant complex flows with the potentially augment bird monitoring capabilities. Leveraging a wind plant deployment, algorithms can be further refined, useful end products developed, and additional technology development can be spurred.

REFERENCES

1. DOE Complex Flows Workshop Report, May 2012.
2. US Patent #9,575,177. Issued February 21, 2017. *Apparatus and Method for Using Radar to Evaluate Wind Flow Fields for Wind Energy* – J. L. Schroeder, J. G. Guynes, and B. D. Hirth. Assignee: Texas Tech University System.
3. US Patent #9,519,056. Issued December 13, 2016. *System and Method for Evaluating Wind Flow Fields Using Remote Sensing Devices* – J. L. Schroeder, B. D. Hirth, and J. G. Guynes. Assignee: Texas Tech University System.
4. Hirth, B. D., J. L. Schroeder, W. S. Gunter, and J. G. Guynes (2012). "Measuring a Utility-Scale Turbine Wake Using the TTUKa Mobile Research Radars." *J. Atmos. Oceanic Technol.*, 29, 765–771.
5. Hirth, B. D., and J. L. Schroeder (2013). "Documenting Wind Speed and Power Deficits behind a Utility-Scale Wind Turbine." *J. Appl. Meteor. Climatol.*, 52, 39-46.
6. Hirth, B. D., J. L. Schroeder, S. W. Gunter, and J. Guynes (2014). "Coupling Doppler Radar-derived Wind Maps with Operational Turbine Data to Document Wind Farm Complex Flows." *Journal of Wind Energy*, 18, 529-540.
7. Hirth B. D., J. L. Schroeder, Z. Irons, and K. Walter (2015). "Case Study: Dual-Doppler Measurements of a Wind Ramp Event at an Oklahoma Wind Plant." *Journal of Wind Energy*, 19, 953-962.
8. Marathe, N., A. Swift, B. Hirth, R. Walker, and J. L. Schroeder (2015). "Characterizing Power Performance and Wake of a Wind Turbine under Yaw and Blade Pitch." *Journal of Wind Energy*, 19, 963-978.
9. Lundquist, J. K.,J. M. Wilczak, R. Ashton, L. Bianco, W. A. Brewer, A. Choukulkar, A. J. Clifton, M. Debnath, R. Delgado, K. Friedrich, S. Gunter, A. Hamidi, G. V. Iungo, A. Kaushik, B. Kosović, P. Langan, A. Lass, E. Lavin, J. C.-Y. Lee, K. L. McCaffrey, R. K. Newsom, D. C. Noone, S. P. Oncley, P. T. Quelet, S. P. Sandberg, J. L. Schroeder, W. J. Shaw, L. Sparling, C. St. Martin, A. St. Pe, E. Strobach, K. Tay, B. J. Vanderwende, A.Weickmann, D. Wolfe, and R. Worsnop (2016). "Assessing State-of-the-Art Capabilities for Probing the Atmospheric Boundary Layer: the XPIA Field Campaign." *Bulletin of the American Meteorological Society*, DOI: 10.1175/BAMS-D-15-00151.1, In Press.
10. Shambayati, S. (2008). "Atmosphere Attenuation and Noise Temperature at Microwave Frequencies." *Low-Noise Systems in the Deep Space Network,* MacGregor S. Reid, Ed., John Wiley and Sons, 255-280.
11. Battan, L. J. (1973). *Radar Observations of the Atmosphere*. University of Chicago Press, 324 pp.
12. Martin, J. M., and A. Shapiro (2007). "Discrimination of Bird and Insect Radar Echoes in Clear Air Using High-Resolution Radars." *J. Atmos. Oceanic Technol.*, 24, 1215-1230.